

CrystEngComm

rsc.li/crystengcomm



ISSN 1466-8033



Cite this: *CrystEngComm*, 2022, 24, 2213

Received 18th February 2022,
Accepted 3rd March 2022

DOI: 10.1039/d2ce00232a

rsc.li/crystengcomm

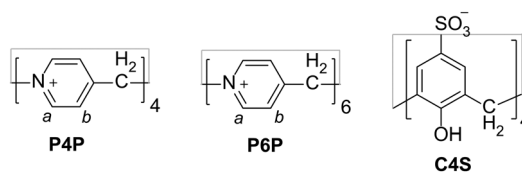
Cationic pillar[*n*]pyridiniums and anionic *p*-sulfonatocalix[4]arene co-assemble into all-organic supersalts through encaging of the supercation units within/between the capsules that emerge from superanion pairs. The encapsulation occurs both in the solid state and in solution and allows the base-sensitive cationic pillar[*n*]pyridiniums to survive under otherwise destructive conditions. This property of supersalts makes them promising repositories for chemically vulnerable charged entities.

Electrostatic interactions play a key role in supramolecular chemistry, and they are also central to biology as the majority of biological macromolecules bear a charge which helps to regulate their functions. For example, DNA is negatively charged, proteins can be positively or negatively charged depending on the pH, *etc.*¹ While Nature has mastered the rules of directed self-assembly in water and biological fluids, the assembly of synthetic molecular building blocks towards predictable complex architectures in an aqueous environment is still a challenge. Introduction of multiple charged functionalities into various macrocyclic platforms is an attractive strategy for fostering polyvalent interactions between assembling components and providing aqueous solubility.² Besides fundamental host-guest chemistry, macrocyclic hosts such as calix[*n*]arenes, cucurbit[*n*]urils and cyclodextrins have been richly exploited to design large, well organized assemblies and architectures, like supramolecular polymers,³ micelles,⁴ vesicles,⁵ giant polyhedra⁶ and supramolecular frameworks.⁷ We report here an aqueous self-assembly driven by the complementarity in charge and shape between two families of oligocharged macrocyclic hosts – cationic pillar[*n*]pyridiniums and anionic *p*-sulfonatocalix[4]arene.

Electrostatic co-assembly of pillar[*n*]pyridiniums and calix[4]arene in aqueous media†

Kateryna Kravets, Mykola Kravets, Helena Butkiewicz, Sandra Kosiorek, Volodymyr Sashuk * and Oksana Danylyuk *

Pillar[*n*]pyridiniums (**P[*n*]Ps**) are permanently charged cationic macrocycles of electron-deficient cavities, now available in two sizes – the rigid square-shape tetramer (**P4P**)⁸ and the flexible roughly hexagonal hexamer (**P6P**) (Scheme 1).⁹ **P[*n*]Ps** have been shown to act as versatile nanoreceptors for the visual detection and differentiation of aromatic and linear fatty diacids.¹⁰ Anionic *p*-sulfonatocalix[4]arene (**C4S**) is a key player in aqueous supramolecular chemistry and crystal engineering, with tremendous applications ranging from simple host-guest systems¹¹ to sophisticated drug delivery ensembles,¹² sensors,¹³ vesicles,¹⁴ crystals,¹⁵ and in interactions with proteins,¹⁶ to name a few. Given the propensity of **P[*n*]Ps** to trap water wires or clusters^{8,9} and of **C4S** to include intracavity water molecules *via* non-conventional OH⋯π hydrogen bonding,¹⁷ we anticipated a peculiar interplay between their combined supramolecular cavities and water molecules. Interestingly, our hybrid pillar[*n*]pyridinium/calix[4]arene systems are devoid of any coordination or classical hydrogen bonding interactions between macrocyclic components, rendering the assembly guided, besides electrostatic attraction, by less conventional interactions, such as anion⋯π⁺, anion⋯π⁺⋯anion, and π⋯π⁺. We show that such self-assembly is indeed feasible and provides a useful pathway to create hybrid co-assemblies built from oppositely charged macrocycles in aqueous media. We also discuss the ability of the co-assemblies to improve the chemical stability of **P[*n*]Ps** both in solution and in the solid state.



Scheme 1 Chemical structure of pillar[4]pyridinium (**P4P**), pillar[6]pyridinium (**P6P**), and *p*-sulfonatocalix[4]arene (**C4S**).

Institute of Physical Chemistry, Polish Academy of Sciences, Kasprzaka 44/52, 01-224 Warsaw, Poland. E-mail: odanylyuk@ichf.edu.pl

† Electronic supplementary information (ESI) available: Experimental details, additional figures, and X-ray crystallographic files in CIF format. CCDC 2127199 and 2127200. For ESI and crystallographic data in CIF or other electronic format see DOI: 10.1039/d2ce00232a



P4P and **C4S** are a perfect match in terms of charge, shape, and symmetry. Both macrocycles have good solubility in water. However, mixing of their aqueous solutions results in rapid clouding and precipitation of white microcrystals. This demonstrates a very strong interaction rapidly leading to a product of much lower solubility than the starting components of the assembly. In order to slow down the formation of a new low-soluble phase, we turned our attention to the replacement of the self-assembly and crystallization environment from aqueous solution to agarose hydrogel medium. Crystallization in gel has long been recognized as a simple, effective, and inexpensive method for improving the quality of single crystals, for tuning the crystal size and morphology, for the inhibition or promotion of nucleation, and even for the control of crystal forms.¹⁸ As a crystallization set-up we used a U-tube filled with agarose gel with one arm filled with an aqueous solution of **P4P** and another arm with a solution of **C4S**. Such crystallization involving diffusion of each macrocyclic component through the gel medium succeeded in obtaining yellow single crystals of the product. The crystals were recovered manually from gel and characterized by single crystal X-ray diffraction. The isolated solid form is a highly symmetric complex of **P4P** with **C4S** ($P4_2/m$ space group) of 1:1 stoichiometry as can be expected from perfect charge complementarity. However, two different ways of complexation between macrocyclic components are manifested in the crystalline assembly, as shown in Fig. 1A. First is the inclusion capsular arrangement of two **C4S** molecules holding one **P4P** (colored in cornflower blue) with entrapped water molecules (Fig. 1B). One of the water molecules O2W sits exactly in the center of the small **P4P** cavity at the intersection of the mirror plane and the two-fold rotation axis (Fig. 1C). This intracavity water molecule is in the same distance from all four pyridinium walls of **P4P** suitable for O–H \cdots π^+ hydrogen bonding. The O \cdots centroid distances of 3.10 Å are surprisingly short, even shorter than the O–H \cdots π hydrogen bonds between intracavity water molecules embedded into **C4S**, as determined from neutron diffraction data (3.12–3.15 Å).^{17b} Two other water molecules reside over each rim of the **P4P** macrocyclic box interacting with the intracavity water molecule *via* O–H \cdots O HB (2.73 Å) in the nearly linear arrangement (Fig. 1D). The electron-deficient skeleton of **P4P** interacts with the electron-rich inner walls of **C4S** and its anionic upper rim *via* a set of non-conventional interactions (Fig. 1E). There are anion \cdots π^+ short contacts between two opposite sulfonate groups of **C4S** and two π^+ aromatic systems of **P4P**, with O(sulfonate) \cdots C(pyridinium) distances in the range of 2.93–3.22 Å. The interaction energies of such anion– π^+ complexes are known to be dominated by strong electrostatic effects exhibiting very large binding energies.¹⁹ Additionally, the $\pi\cdots\pi^+$ interaction between the aromatic walls of **C4S** and **P4P** (the interplane separation being 3.57 Å) reinforce the capsular assembly. Also, (C–H) $^+\cdots\pi$ and (C–H) $^+\cdots$ O $^-$ interactions between methylene and pyridinium (C–H) $^+$ donors of **P4P** and electron-rich aromatic systems or sulfonate oxygen atoms of

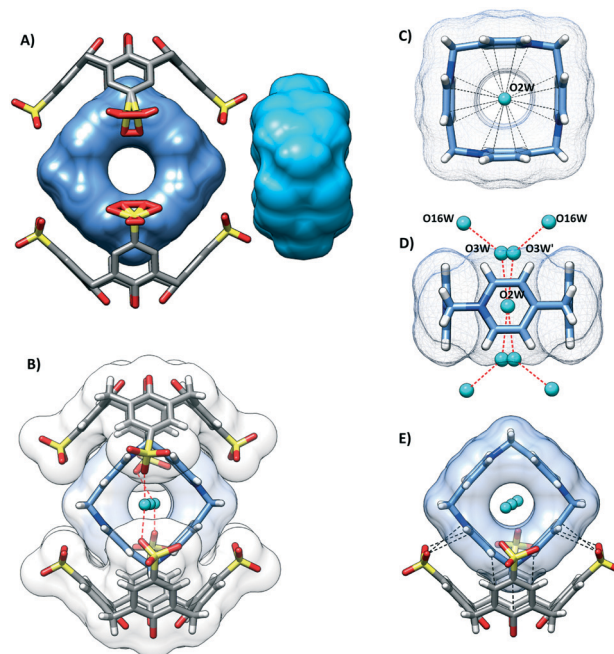


Fig. 1 A) Expanded asymmetric unit of the **P4P**–**C4S** co-assembly, wherein two crystallographically non-equivalent **P4P** are colored in cornflower blue and sky blue, and all water molecules have been omitted for clarity; B) capsular 1:2 **P4P**–**C4S** ensemble with trapped water molecules (in cyan) inside the **P4P** cavity; C) water molecule in the exact center of the **P4P** cavity interacting with electron-deficient pyridinium walls of **P4P**, wherein the O \cdots centroid distances are of 3.10 Å; D) the expansion of a hydrogen bonded network around an intracavity water molecule; E) anion $\cdots\pi^+$ and (C–H) $^+\cdots\pi$ interactions between **C4S** and **P4P** (in black dashed lines); $\pi\cdots\pi^+$ interactions between **C4S** electron-rich and **P4P** electron-deficient rings are not shown for clarity.

C4S contribute to the complexation. Another crystallographically independent **P4P** (colored in sky blue) resides in the cage formed by exo-walls of four **C4S** molecules (Fig. S1†). The complexation is again realized *via* a set of anion $\cdots\pi^+$, $\pi\cdots\pi^+$, and (C–H) $^+\cdots$ O $^-$ interactions. The center of the **P4P** cavity is also occupied by a water molecule.

The crystallization of the larger hexacationic **P6P** with **C4S** posed a similar challenge of charge-neutralization induced precipitation. In this case the liquid–liquid diffusion of layered aqueous solutions of **C4S** and **P6P** in the NMR tube has been successfully applied to slow down nucleation and obtain single crystals of the **P6P**–**C4S** complex. Single crystal X-ray diffraction revealed the 2:3 **P6P**–**C4S** co-assembly to be in the $P\bar{1}$ space group, comprising 2 **P6P** hexacations and 3 **C4S**, Fig. 2A tetraanions. Again, there are two modes of complexation in the solid state: two **C4S** molecules hold one **P6P** molecule in the capsule-type arrangement, and one **C4S** molecule shroud one **P6P** molecule in the open geometry. Interestingly, the **P6P** conformation is different from the honeycomb columnar shape with all the aromatic walls aligned. Such a columnar conformation was previously confirmed in the up to now solely reported crystal structure of **P6P** in the form of its hexachloride salt hydrate.⁹ Here, the



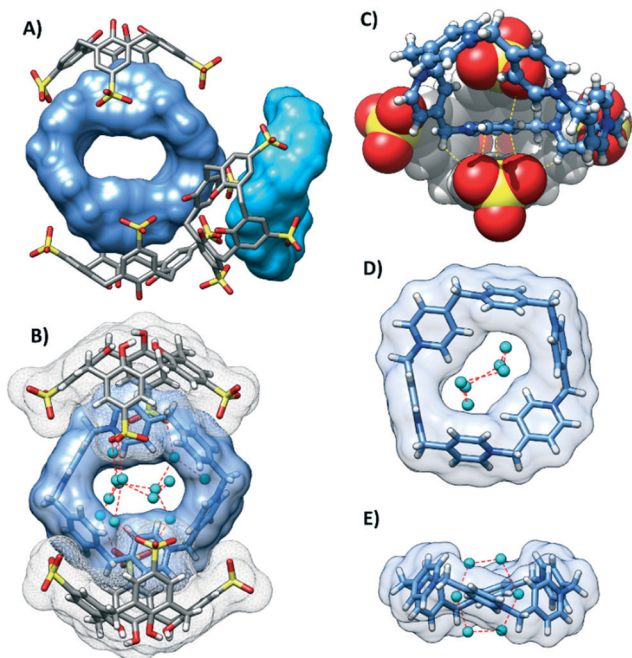


Fig. 2 A) Asymmetric unit of the **P6P-C4S** co-assembly, wherein two crystallographically non-equivalent **P6P** are colored in cornflower blue and sky blue, and all water molecules have been omitted for clarity; B) capsular 1:2 **P6P-C4S** ensemble with included and surrounded water molecules (in cyan); C) anion $\cdots\pi^+$ and (C-H) $^+\cdots\text{O}^-$ interactions between **C4S** and **P6P** (in yellow dashed lines); $\pi\cdots\pi^+$ interactions between **C4S** electron-rich and **P6P** electron-deficient rings are not shown for clarity; D) hexameric ice-like water cluster included in the **P6P** cavity; E) side view of the **P6P** and trapped water cluster.

P6P nanoring in the capsular assembly is significantly distorted from the columnar geometry with two opposite aromatic rings oriented roughly perpendicular with respect to their neighboring walls (Fig. 2B). Such a distorted conformation of **P6P** is similar to the theoretically predicted saddle-like **P6P** geometry in aqueous solution.⁹ Two twisted aromatic walls of **P6P** are inserted into pinched cone **C4S** cavities suitable for anion- π^+ sandwiching (Fig. 2C). The O(sulfonate) \cdots C(pyridinium) distances are in the range of 3.01–3.33 Å (the O $^-$ \cdots centroid distances in the anion- π^+ sandwich are 3.08 and 3.15 Å). The (C-H) $^+\cdots\pi$ interactions between methylene and pyridinium (C-H) $^+$ donors of **P4P** and electron-rich aromatic systems of **C4S** contribute to the complexation. The central elongated hole of **P6P** is occupied by 6 water molecules in an ice-like chair arrangement, (Fig. 2D and E). Two of these water molecules reside in the central part of the cavity and are in close contact with four internal pyridinium walls evidencing O-H $\cdots\pi^+$ interactions, with O \cdots centroid distances in the range of 3.00–3.34 Å. The hexameric water clusters are not isolated, but hydrogen bonded to more water molecules surrounding the capsular assembly and to sulfonate groups of the **C4S** molecules. Another type of complexation is the 1:1 open complex, with **P6P** in a different conformation, in which all pyridinium rings are twisted alternately in and out from the macrocycle plane (Fig. S2 †). While the **P6P** position is almost vertical in

the capsular assembly, here the **P6P** is arranged slant-wise with respect to **C4S** molecular axes. This assembly is also spanned and surrounded by multiple water molecules; however, detailed analysis of the interaction mode is hampered by heavy disorder of **P6P** and water molecules.

Having established the structure of the supersalts, we proceeded to the study of the chemical properties of the co-assembled components. Whereas **C4S** can generally be considered chemically resistant, **P[n]Ps**, like other pyridinium containing macrocycles,²⁰ are prone to deprotonation, which ultimately leads to irreversible structural changes and limits their application scope. We wondered if the co-assembly of **P[n]Ps** with **C4S** can improve their chemical stability. We prepared crystalline powders of **P4P**, **P6P**, and their complexes with **C4S**,

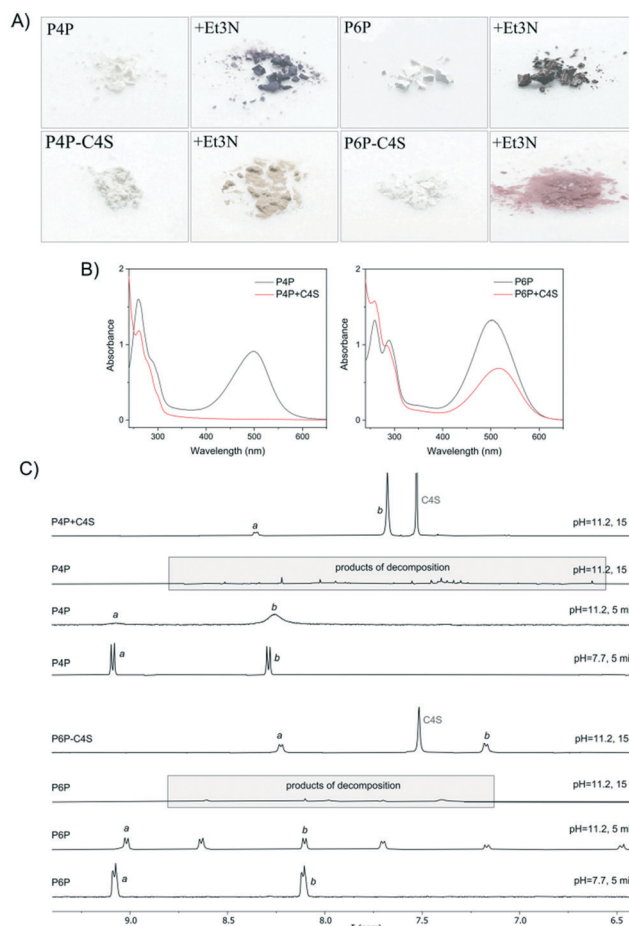


Fig. 3 A) Photographs of the powders of **P[n]Ps** and their complexes with **C4S** before (left) and after dropping triethylamine (right); B) UV-vis spectra of **P[n]Ps** and their mixtures with **C4S** (1.5 eq.) in 0.8 M Tris buffer (pH \approx 11.2). A signal with a maximum close to 500 nm corresponds to the deprotonation and is responsible for the red color seen by the naked eye; C) partial ^1H NMR spectra of the solutions of **P[n]Ps** and their mixtures with **C4S** (1.5 eq.) in 0.8 M Tris buffer (pH \approx 11.2). For comparison, the spectra of **P[n]Ps** at near neutral pH are also shown. While free macrocycles practically completely decompose after 15 h, the complexed **P[n]Ps** remain intact. The acquired chemical resistance can be accounted for by the encapsulation of the cationic macrocycles within **C4S** cavities manifested by large upfield shifts of proton resonances belonging to **P[n]Ps**.



and treated them with triethylamine, a common organic base ($pK_a = 10.7$). The effect was immediate (Fig. 3A). The initially white neat **P[n]P** powders instantaneously turned dark, while the same colored **C4S** samples remained almost unchanged (**P4P**) or changed slightly (**P6P**). The visual differences between **P4P** (pale yellow) and **P6P** (pink, indicating deprotonation) correlate well with the base's access to each macrocycle in the crystal lattice. Smaller and better protected **P4P** is evidently less reactive than larger and more exposed **P6P**. The same behavior can be seen in the solution. While the alkaline aqueous solution of **P4P** mixed with **C4S** ($pH \approx 11.2$) shows no sign of deprotonation, **P6P** under the same conditions deprotonates to some degree (Fig. 3B). Importantly, co-assembly with **C4S** not only attenuates or even ceases the deprotonation but also helps to avoid the decomposition, which is observed over time for the unprotected **P[n]Ps** (Fig. 3C). Such a marked change in reactivity can be rationalized by the encapsulation of **P[n]P** macrocycles within the **C4S** cavity that takes place both in the solid state and in solution.

In conclusion, pillar[n]pyridiniums and *p*-sulfonatocalix[4]arene co-assemble in aqueous media through encaging of the cationic pillar[n]pyridinium units within/between the capsules that emerge from superanion calix[4]arene pairs. The decisive supramolecular forces responsible for the co-assembly and supramolecular architecture are electrostatic attractions between oppositely charged macrocycles combined with specific anion $\cdots\pi^+$, anion $\cdots\pi^+\cdots$ anion, and $\pi\cdots\pi^+$ interactions. The con-shaped calix[4]arene cavity serves as host for the cationic pillar[n]pyridiniums in both co-assemblies, while pillar[n]pyridinium cavities are further filled with either a single water molecule in **P4P** or a hexameric water cluster in **P6P**. The encaging and protection of pillar[n]pyridiniums by calix[4]arene take place both in the solid state and in solution, and this allows the base-sensitive cationic macrocycles to survive under otherwise destructive conditions. This ability of supramolecular supersalts to improve the chemical stability of pillar[n]pyridiniums makes them promising repositories for chemically pregnable charged entities.

This project was funded by the National Science Centre of Poland (grant PRELUDIUM BIS-1 no. 2019/35/O/ST4/01865).

Conflicts of interest

There are no conflicts to declare.

Notes and references

- (a) B. Honig and A. Nicholls, *Science*, 1995, **268**, 1144; (b) A. G. Cherstvy, *Phys. Chem. Chem. Phys.*, 2011, **13**, 9942.
- (a) N. K. Beyeh, Nonappa, V. Liljestrom, J. Mikkila, A. Korpi, D. Bochicchio, G. M. Pavan, O. Ikkala, R. H. A. Ras and M. A. Kostiaainen, *ACS Nano*, 2018, **12**, 8029; (b) N. M. Mockler, K. O. Ramberg, F. Guagnini, C. L. Raston and P. B. Crowley, *Cryst. Growth Des.*, 2021, **21**(3), 1424; (c) M. L. Rennie, A. M. Doolan, C. L. Raston and P. B. Crowley, *Angew. Chem., Int. Ed.*, 2017, **56**, 5517.
- X. Ji, M. Ahmed, L. Long, N. M. Khashab, F. Huang and J. L. Sessler, *Chem. Soc. Rev.*, 2019, **48**, 2682.
- (a) S. Fujii, Y. Sanada, T. Nishimura, I. Akiba, K. Sakurai, N. Yagi and E. Mylonas, *Langmuir*, 2012, **28**(6), 3092; (b) K. Suwinska, B. Leśniewska, M. Wszelaka-Rylik, L. Straver, S. Jebors and A. W. Coleman, *Chem. Commun.*, 2011, **47**, 8766.
- T. Xiao, W. Zhong, L. Xu, X.-Q. Sun, X.-Y. Hu and L. Wang, *Org. Biomol. Chem.*, 2019, **17**, 1336.
- S. Pasquale, S. Sattin, E. C. Escudero-Adán, M. Martínez-Belmonte and J. de Mendoza, *Nat. Commun.*, 2012, **3**, 785.
- (a) Y. Zhou, K. Jie, R. Zhao and F. Huang, *Adv. Mater.*, 2020, **32**, 1904824; (b) S. Lim, H. Kim, N. Selvapalam, K. J. Kim, S. J. Cho, G. Seo and K. Kim, *Angew. Chem., Int. Ed.*, 2008, **47**(18), 3352.
- S. Kosiorek, B. Rosa, T. Boinski, H. Butkiewicz, M. P. Szymański, O. Danylyuk, A. Szumna and V. Sashuk, *Chem. Commun.*, 2017, **53**, 13320.
- S. Kosiorek, H. Butkiewicz, O. Danylyuk and V. Sashuk, *Chem. Commun.*, 2018, **54**, 6316.
- (a) M. Kravets, G. Sobczak, N. Rad, I. Misztalewska-Turkiewicz, O. Danylyuk and V. Sashuk, *Chem. Commun.*, 2020, **56**, 8595; (b) M. Kravets, I. Misztalewska-Turkiewicz and V. Sashuk, *Sens. Actuators, B*, 2021, **343**, 130083.
- D.-S. Guo and Y. Liu, *Acc. Chem. Res.*, 2014, **47**(7), 1925.
- W.-C. Geng, J. L. Sessler and D.-S. Guo, *Chem. Soc. Rev.*, 2020, **49**, 2303.
- D.-S. Guo, V. D. Uzunova, X. Su, Y. Liu and W. M. Nau, *Chem. Sci.*, 2011, **2**, 1722.
- S. Peng, K. Wang, D.-S. Guo and Y. Liu, *Soft Matter*, 2015, **11**, 290.
- (a) M. J. Hardie and C. L. Raston, *J. Chem. Soc., Dalton Trans.*, 2000, 2483; (b) J. L. Atwood, L. J. Barbour, M. J. Hardie and C. L. Raston, *Coord. Chem. Rev.*, 2001, **222**, 3; (c) S. J. Dalgarno, J. L. Atwood and C. L. Raston, *Chem. Commun.*, 2006, 4567; (d) O. Danylyuk and K. Suwinska, *Chem. Commun.*, 2009, 5799.
- (a) F. Perret and A. W. Coleman, *Chem. Commun.*, 2011, **47**, 7303; (b) R. E. McGovern, A. A. McCarthy and P. B. Crowley, *Chem. Commun.*, 2014, **50**, 10412.
- (a) J. L. Atwood, F. Hamada, K. D. Robinson, G. W. Orr and R. L. Vincent, *Nature*, 1991, **349**, 683; (b) K. Fucke, K. M. Anderson, M. H. Filby, M. Henry, J. Wright, S. A. Mason, M. J. Gutmann, L. J. Barbour, C. Oliver, A. W. Coleman, J. L. Atwood, J. A. K. Howard and J. W. Steed, *Chem. – Eur. J.*, 2011, **17**, 10259.
- D. K. Kumar and J. W. Steed, *Chem. Soc. Rev.*, 2014, **43**, 2080.
- J. J. Fiol, M. Barceló-Oliver, A. Tasada, A. Frontera, À. Terrón and Á. García-Raso, *Coord. Chem. Rev.*, 2013, **257**, 2705.
- W. R. Dichtel, O. Š. Miljanić, J. M. Spruell, J. R. Heath and J. F. Stoddart, *J. Am. Chem. Soc.*, 2006, **128**(32), 10388.

